IEEE Access
Multidisciplinary | Rapid Review | Open Access Journal

Received May 20, 2021, accepted May 31, 2021, date of publication June 7, 2021, date of current version June 15, 2021.

Digital Object Identifier 10.1109/ACCESS.2021.3087223

Perfect Control for Continuous-Time LTI State-Space Systems: The Nonzero Reference Case Study

PAWEŁ MAJEWSKI, WOJCIECH P. HUNEK, AND MAREK KROK
Department of Control Science and Engineering, Opole University of Technology, 45-758 Opole, Poland
Corresponding author: Paweł Majewski (p.majewski@po.edu.pl)

ABSTRACT In this paper an innovative study concerning the perfect control algorithm is presented. This particular control strategy has already been developed for continuous- and discrete-time transfer-function-originated plants, as well as discrete-time state-space-related systems, however the approach devoted to continuous-time state-space objects is still an unexplored research area. With the application of the time-dependent system correction joined with nonunique matrix inverses, a new maximum-speed and maximum-accuracy control paradigm is established within this research. Simulation cases performed in the Matlab/Simulink environment show, that the new results can successfully be applied in the field of control theory and practice.

INDEX TERMS Perfect control, continuous-time system, inverse model control, inverses of nonsquare matrices, degrees of freedom, MIMO, practical implementation.

SYMBOLS

$\mathbf{A}$	system matrix
$\mathbf{A}^*$	closed-loop system matrix
$\mathbf{B}$	input matrix
$\mathbf{C}$	output matrix
dt	continuous step time
F_x, F_y, F_z	forces of respective axes
$\mathbf{f}(t)$	any continuous-time function
g	gravity acceleration
$\mathbf{I}$	identity matrix
$J(.)$	performance index
$\mathbf{K}$	state-feedback matrix
k	index
k_x, k_y, k_z	viscous friction coefficients of respective axes
L	difference between kinetic and potential energies
$\mathbf{M}$	perfect control-originated matrix
m	scalar value of matrix $\mathbf{M}$
m_1, m_2, m_3	masses of robot's links
n	number of state variables
n_u	number of inputs
n_y	number of outputs
q^{-1}	backward shift operator
q_x, q_y, q_z	gripper tip position in XYZ-coordinates
s	continuous Laplace operator
T, U	kinetic and potential energy, respectively
t	continuous time
$\mathbf{U}, \mathbf{V}$	SVD-related matrices
$\mathbf{u}(t)$	input vector in t
$\mathbf{x}(t)$	state vector in t
$\mathbf{x}_0, \mathbf{x}(0)$	initial state vector
$\mathbf{y}(t)$	output vector in t
$\mathbf{y_{ref}}(t)$	reference value/setpoint in t
β	degrees of freedom matrix
Σ	SVD eigenvalue matrix
$(.)^{\mathrm{L}}$	any generalized left inverse
$(.)^{\mathrm{R}}$	any generalized right inverse
$(.)_0^{\mathrm{R}}$	minimum-norm right inverse
$(.)^{\mathrm{T}}$	transpose symbol
$\dot{(.)}$	derivative symbol
$(.)^{-1}$	regular matrix inverse
$\underline{(.)}$	polynomial matrix in q^{-1}

ABBREVIATIONS

BIBO	Bounded-Input, Bounded-Output
BIBS	Bounded-Input, Bounded-State

The associate editor coordinating the review of this manuscript and approving it for publication was Wence Zhang.

CTPC	Continuous-Time Perfect Control
IMC	Inverse Model Control
LTI	Linear Time-Invariant
MIMO	Multiple-Input, Multiple-Output
SVD	Singular Value Decomposition

I. INTRODUCTION

Modern control algorithms often entail a numerical complexity and usually are connected with mathematical challenges such as nonuniqueness or inverse problem [1]–[4]. It should be emphasized, that both of these peculiarities have strongly been addressed to the inverse model control framework [5]–[7]. The parameter and polynomial matrix inverses constitute a self-standing scientific area, which gathered a reasonable interest during past years [8]–[10]. For instance, the inverse-based pole-free perfect control for discrete-time state-space system has already been delivered in such a way [11]. Notwithstanding, the inverse problem has nonunique solutions mainly for plants having plural numbers of inputs and outputs [12]–[14]. This phenomenon is employed during design of IMC robust MIMO strategies [7], [15].

The multivariable systems, i.e. plants with different number of input and output variables, has collected considerable attention over past years [7], [11]. This is due to the fact that most challenges have multiple nonunique solutions, thus additional benefits can be obtained apart from those associated with minimizing the main goal functions. For example, the control energy can be optimized with presumed output behavior during different control actions [16], [17]. Moreover, the multivariable control design is often connected with a matrix calculation, since the matrix-based state-space description is preferable in those considerations.

One of control strategies benefiting from both multivariability and matrix-based nature is the perfect control algorithm. For now, this control scheme is well-described for deterministic discrete-time plants with remarkable almost zero-error performance [4]. Moreover, thanks to the nonuniqueness occurring in this inverse-model-based scenarios, some additional properties were assigned to the perfect control systems. Just to mention, the main improvements were obtained using the nonunique matrix inverses applied to the perfect control design process [11].

As already indicated, the area of matrix inverses is yet another interesting topic worth of a scientific discussion [18]. In the context of perfect control design, there is a wide history of development and implementations of inverse-based studies in the field of modern control theory. For years, the Moore-Penrose inverse has been used during different theoretical and practical tasks according to its minimum-norm property [19], [20]. This specific inverse is said to guarantee unique and 'best' reachable solution. However, it has recently revealed, that in several applications there is a possibility to withstand the Moore-Penrose inverse dominance. For instance, the nonunique right σ-inverse (or H-inverse) has shown its overwhelming reliability in stabilizing the inverse-based perfect controller [11]. Moreover, a plethora of different inverses have been investigated in past years, thus the selection of the proper one becomes more and more complex task.

Notwithstanding, most of the mentioned peculiarities have been used in the discrete-time manner, as the perfect control is well known for such system framework (for example see Ref. [14] in the context of new energy-based criterion dedicated to discrete-time perfect control law). What could have been foreseen, the discussed control law obtained for discrete-time systems applied to the continuous-time plant resulted in the odd responses of the steady-state values, but different from the reference ones. Thus, the correction module has to be introduced to obtain the proper perfect control response. Therefore, the process of continuous-time perfect control system design with the application of nonsquare matrix inverses constitutes the main matter of this work. The novelty and complexity of continuous-time perfect control algorithm applied to the continuous-time plants seems to be yet unexplored and valuable theory area never seen before. Of course, this scenario is connected with a very high energy injection, however instances of such approach can be found in practical applications. In various tasks, there is a need to use the Dirac-oriented control paradigm, where injection of energy is demanded. For example, such devices like satellites or very complex walking systems of humanoid robots can be considered as well [21], [22]. Last but not least, since the proposed approach is certainly associated with the nonsquare MIMO plants, the technical contribution of the IMC-originated solution addressed to the real-life objects should strongly be indicated. At the beginning, the most important chemical engineering industry has to be mentioned, where the nonsquare system issue has probably been firstly raised. The distillation column [23], [24], Shell control problem [25], crude distillation process [26], mixing tank process [27], continuous stirred tank reactor [28] and chemical-mechanical polishing process [29] can constitute the main goal of our investigation. The discussed new method can also be applied to the signal processing branch covering the environmental MIMO structures. In such a case, the desirable dynamic properties are guaranteed through the closed-loop control applications. The so-called perfectualization of the error-control coding [30], precoding and equalization [31], signal reconstruction [32], deconvolution [33] and image recovery [34] seem to be good examples towards the perfect control considerations. On the other hand, the tasks of the perfect reconstruction of signal [35] and minimum variance/perfect control of computer networks [36] as well as the inverse kinematic problem [37] have already become a fact. Finally, the extension in the form of generalized minimum variance control is also observed in the practice [38].

In the end, it is worth mentioning, that the perfect control design process for the continuous-time plants can often be very different from its discrete-time or fractional-order versions [7], [39], [40]. Thus, in this manuscript a comparison

of discrete- versus continuous-time perfect control is made through this study, as the invaluable supplement.

Taking into account all the presented reasons, the paper is organized as follows. After a short introduction, the LTI MIMO continuous-time state-space framework is briefly reminded. It is worth emphasizing, that the system description is crucial in all model-based control scenarios. Later, in Section III, a short explanation of nonunique matrix inverse idea is given together with explicit formulas allowing us to obtain an infinite number of generalized inverses. The main goal of this paper covering the continuous-time perfect control (CTPC) is given in Section IV. Next, in Section V a discussion over stability of such control plants is performed. Some points are given in order to assess the proper new stability criterion. Simulation examples of Section VI show, that the perfect control formula can be successfully applied to continuous-time systems. Two representative theoretical and practical scenarios directly certify the CTPC procedure in the best way. The final conclusions and open problems are included in the closing section of the manuscript.

II. SYSTEM REPRESENTATION

In the paper we are considering an LTI state-space system in continuous-time domain as follows

$$\begin{cases} \dot{\mathbf{x}}(t) = \mathbf{A}\mathbf{x}(t) + \mathbf{B}\mathbf{u}(t), \quad \mathbf{x}(0) = \mathbf{x}_0 \\ \mathbf{y}(t) = \mathbf{C}\mathbf{x}(t), \end{cases} \tag{1}$$

where $\mathbf{A} \in \mathbb{R}^{n\times n}$, $\mathbf{B} \in \mathbb{R}^{n\times n_u}$ and $\mathbf{C} \in \mathbb{R}^{n_y\times n}$ are system, input and output matrices, respectively, whilst $\mathbf{u}(t)$, $\mathbf{y}(t)$ and $\mathbf{x}(t)$ denote the respective n_u-input, n_y-output and n-state vectors. Described plant has the initial state values expressed as $\mathbf{x}_0$ vector equivalent to the $\mathbf{x}(t)$ for $t = 0$.

Remark 1: Because of the nature of the perfect control law, we rather omit the systems with $n_u < n_y$. For such plants it is shown, that the perfect control algorithm cannot be established (for instance see Ref. [4]).

The subsequent Fig. 1 should help to understand the whole setup of the manuscript. Naturally, the proposed scheme is in relation with all simulation instances of Section VI.

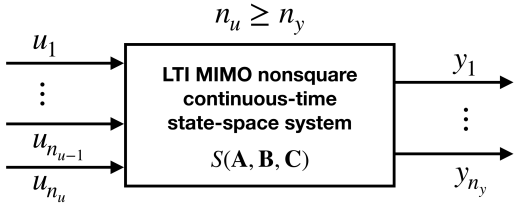

FIGURE 1. The acceptable right-invertible system scenario.

Remark 2: In order to clarify the used nomenclature, it should strongly be noticed that our mathematical investigation covers the continuous time t as the numerical sequence $t_k = t_{k-1} + dt$, with $k = 1, 2, 3 \ldots$, under $dt \to 0$.

The stability of continuous-time plants is clearly connected with the location of system poles. The well-known formula allowing us to determine the main property of a control system is reminded by the following relation

$$det(s\mathbf{I} - \mathbf{A}^*) = 0, \tag{2}$$

with the final stability requirement expressed as $Re(s_i) < 0$ for all i-th roots of the characteristic equation.

Having the fundamental notion of the touched systems, let us now briefly present the crucial nonunique inverses in the next section.

III. NONUNIQUE σ-INVERSES

During the design process of inverse model control schemes, in particular the perfect control systems, there are several main concerns. The first one is the right-invertibility of considered plants. Only for objects with $n_u \geq n_y$, the mentioned control procedure results in a desired system output behavior. In the past, the unique Moore-Penrose inverse has mostly been used, due to its so-called minimum-norm property [41]–[44]. This specific inverse dedicated to polynomial approach is called T-inverse and sounds as follows

$$\underline{\mathbf{B}}_0^{\mathrm{R}}(q^{-1}) = \underline{\mathbf{B}}^{\mathrm{T}}(q^{-1})[\underline{\mathbf{B}}(q^{-1})\underline{\mathbf{B}}^{\mathrm{T}}(q^{-1})]^{-1}, \tag{3}$$

where matrix polynomial $\underline{\mathbf{B}}(q^{-1})$ is of dimension $m \times n$. Thus, the expression (3) constitutes a solid background for other inverses. It is also worth mentioning, that for parameter matrices, the right Moore-Penrose inverse reduces to the parameter matrix form

$$\mathbf{B}_0^{\mathrm{R}} = \mathbf{B}^{\mathrm{T}}(\mathbf{B}\mathbf{B}^{\mathrm{T}})^{-1}, \tag{4}$$

with $\mathbf{B}$ being of the same sizes as $\underline{\mathbf{B}}(q^{-1})$.

Observe, that in the case covering $n_u > n_y$, there is a possibility to obtain an infinite number of different nonunique inverses. As the mentioned topic is a self-standing research area, only the right σ-inverse will be recalled here. This particular inverse is proven to be useful in terms of pole placement, energy optimization or widely understood robustification [11]. The crucial merit of nonunique inverses are the so-called degrees of freedom, which can be observed in the right σ-inverse formula as follows

$$\underline{\mathbf{B}}_{\sigma}^{\mathrm{R}}(q^{-1}) = \underline{\beta}^{\mathrm{T}}(q^{-1})[\underline{\mathbf{B}}(q^{-1})\underline{\beta}^{\mathrm{T}}(q^{-1})]^{-1}, \tag{5}$$

where $\underline{\mathbf{B}}_{m\times n}(q^{-1})$ and $\underline{\beta}_{m\times n}(q^{-1})$ are the full normal rank polynomial and degrees of freedom matrices, respectively.

Remark 3: Of course, similarly to the unique Moore-Penrose inverse, the parameter σ-inverse-originated structure can be obtained here. For matrices without polynomial entries, the nonunique right σ-inverse is in the following form

$$\mathbf{B}_{\sigma}^{\mathrm{R}} = \beta^{\mathrm{T}}(\mathbf{B}\beta^{\mathrm{T}})^{-1}. \tag{6}$$

The σ-inverse can successfully be applied to all state-space-based considerations, since the parameter matrices plays crucial role in this framework.

Nevertheless, any other nonunique inverse can be used in our study. For example, the right H-inverse defined as

$$\mathbf{M}^{\mathrm{R}} = (\mathbf{V}^{\mathrm{T}})^{-1}\Sigma^{\mathrm{R}}\mathbf{U}^{-1}, \tag{7}$$

where operation Σ^{R} allows us to obtain an infinite number of solutions derived from the already mentioned degrees of freedom. Of course, the Singular Value Decomposition (SVD) is used here [45].

The proper definition of nonunique inverses is crucial in the perfect control design, however the generalized inverses are not the main matter of this paper. The development of the perfect control law for continuous-time state-space plants therefor is presented in the next section.

IV. CONTINUOUS-TIME PERFECT CONTROL LAW

The continuous-time perfect control is still a new research area. Observe, that the examined algorithm can be concurrently considering with respect to the following two instances. In the first, more general case, we tell about the nonzero-originated output reference perfect control. On the other hand, the second approach brings us to the reduced zero-setpoint perfect regulation. Below, we start with the simplest solution.

For continuous-time plants described as in (1), the perfect regulation with the zero setpoint can be achieved in just one time increase horizon dt ($\mathbf{y_{ref}}(t+dt)=\mathbf{0}$, $dt\to 0$) according to the following expression

$$\mathbf{u}(t)=\left[-(\mathbf{CB})^{\mathrm{R}}\mathbf{CA}-\frac{\mathbf{B}^{\mathrm{R}}}{dt}\right]\mathbf{x}(t), \tag{8}$$

with symbol $(.)^{\mathrm{R}}$ providing the generalized right inverse.

In order to prove this fact, let's consider any continuous-time function $\mathbf{f}(t)$ together with the subsequent property

$$\mathbf{f}(t_k)=\mathbf{f}(t_{k-1})+\dot{\mathbf{f}}(t_{k-1})dt, \tag{9}$$

where $t_k=t_{k-1}+dt$ and $dt\to 0$. Naturally, the above formula is true for any case, since we have

$$\mathbf{f}(t_{k-1})+\lim_{dt\to 0}\frac{\mathbf{f}(t_k)-\mathbf{f}(t_{k-1})}{dt}dt=\mathbf{f}(t_k). \tag{10}$$

In such scenario, after substitution the control law (8) into the first part of the description (1), we receive

$$\dot{\mathbf{x}}(t)=\left[\mathbf{A}-\mathbf{B}(\mathbf{CB})^{\mathrm{R}}\mathbf{CA}\right]\mathbf{x}(t)-\frac{\mathbf{x}(t)}{dt}, \tag{11}$$

which can be adopted by (9), finally to obtain

$$\mathbf{x}(t_k)=\mathbf{x}(t_{k-1})+\left[\mathbf{A}-\mathbf{B}(\mathbf{CB})^{\mathrm{R}}\mathbf{CA}\right]\mathbf{x}(t_{k-1})dt-\mathbf{x}(t_{k-1}). \tag{12}$$

For $\mathbf{y}(t_k)=\mathbf{Cx}(t_k)$ we immediately confirm our investigation due to

$$\mathbf{y}(t_k)=\mathbf{Cx}(t_{k-1})+\left[\mathbf{CA}-\underbrace{\mathbf{CB}(\mathbf{CB})^{\mathrm{R}}}_{\mathbf{I}_{n_y}}\mathbf{CA}\right]\mathbf{x}(t_{k-1})dt-\mathbf{Cx}(t_{k-1})=\mathbf{0}, \tag{13}$$

where $\mathbf{I}_{n_y}$ stands for the identity matrix.

Of course, this property is not aimed in this paper. It will only be used later to achieve guaranteed steady states. Thus, an effort has been undertaken in order to enable our control strategy to obtain arbitrary output reference and the results which are expected in this paper.

Now, basing on the performance index minimizing the control error

$$J(y)=||\mathbf{y_{ref}}(t)-\mathbf{y}(t)||, \tag{14}$$

where $\mathbf{y_{ref}}(t)$ stands for the reference value, we can perform an attempt to obtain similar minimum-error behavior as observed in the discrete-time approach [11]. The study presented here can be condensed to the essential theorem.

Theorem 1: An arbitrary continuous-time state-space system represented by formulas (1) receives the output value $\mathbf{y}(t+dt)=\mathbf{y_{ref}}(t+dt)$ after one step dt, under $dt\to 0$, with the following perfect control signal

$$\mathbf{u}(t)=\left[-(\mathbf{CB})^{\mathrm{R}}\mathbf{CA}-\mathbf{B}^{\mathrm{R}}\mathbf{M}\right]\mathbf{x}(t), \tag{15}$$

where $\mathbf{M}$ is the specified matrix described by the formula

$$\mathbf{M}=\mathbf{C}^{\mathrm{R}}\frac{1}{dt}\left[\mathbf{Cx}(t_{k-1})-\mathbf{y_{ref}}(t_k)\right]\mathbf{x}^{\mathrm{L}}(t_{k-1}), \tag{16}$$

whereas $(.)^{\mathrm{L}}$ is related to any generalized left inverse.

Proof: After substituting the control law (15) to the expressions (1), we obtain the relation of dynamics as follows

$$\dot{\mathbf{x}}(t)=\left(\mathbf{A}-\mathbf{B}(\mathbf{CB})^{\mathrm{R}}\mathbf{CA}-\mathbf{M}\right)\mathbf{x}(t). \tag{17}$$

Now, basing on the property (9), we can calculate the actual state vector with respect to the past values

$$\mathbf{x}(t_k)=\left(\mathbf{I}_n+\left(\mathbf{A}-\mathbf{B}(\mathbf{CB})^{\mathrm{R}}\mathbf{CA}-\mathbf{M}\right)dt\right)\mathbf{x}(t_{k-1}). \tag{18}$$

Finally, after substitution the received formula to the output of the system (1) we have

$$\begin{aligned}\mathbf{y}(t_k)&=(\mathbf{C}-\mathbf{CM}dt)\,\mathbf{x}(t_{k-1})=\mathbf{Cx}(t_{k-1})-\underbrace{\mathbf{CC}^{\mathrm{R}}}_{\mathbf{I}_{n_y}}\frac{1}{dt}dt\\&\quad*\left[\mathbf{Cx}(t_{k-1})-\mathbf{y_{ref}}(t_k)\right]\underbrace{\mathbf{x}^{\mathrm{L}}(t_{k-1})\mathbf{x}(t_{k-1})}_{\text{unity}}\\&=\mathbf{y_{ref}}(t_k),\end{aligned} \tag{19}$$

where $t_k=t_{k-1}+dt$ for $dt\to 0$ and $\mathbf{M}$ is associated with (16).

□

Remark 4: In case of a system with n-inputs and single-output, the matrix $\mathbf{M}$ can be simplified to the form

$$\mathbf{M}=\mathbf{I}_n*m, \tag{20}$$

where $\mathbf{I}_n$ is the identity matrix and m is a scalar equal to

$$m=\frac{1}{dt}-\mathbf{y_{ref}}(t_k)\left(\mathbf{Cx}(t_{k-1})\right)^{-1}\frac{1}{dt}. \tag{21}$$

Note, that expressions $\mathbf{y_{ref}}(t_k)$ and $(\mathbf{Cx}(t_{k-1}))^{-1}$ are also scalars.

Naturally, in such reduced instance we receive the same result as in general case (19). The confirmation can be written as follows

$$\begin{aligned}\mathbf{y}(t_k) &= (\mathbf{C} - \mathbf{CM}dt)\,\mathbf{x}(t_{k-1}) = \mathbf{Cx}(t_{k-1}) - \mathbf{C}\frac{1}{dt}dt \\ &\quad * [\mathbf{Cx}(t_{k-1}) - \mathbf{y_{ref}}(t_k)]\,(\mathbf{Cx}(t_{k-1}))^{-1}\,\mathbf{x}(t_{k-1}) \\ &= \mathbf{Cx}(t_{k-1}) - \mathbf{Cx}(t_{k-1}) \\ &\quad + \mathbf{Cy_{ref}}(t_k)\,(\mathbf{Cx}(t_{k-1}))^{-1}\,\mathbf{x}(t_{k-1}) \\ &= \mathbf{y_{ref}}(t_k)\,(\mathbf{Cx}(t_{k-1}))^{-1}\,\mathbf{Cx}(t_{k-1}) \\ &= \mathbf{y_{ref}}(t_k). \end{aligned} \tag{22}$$

Remark 5: Let's discuss yet the performance index value delivered by the algorithm presented in this paper. Therefore, after assuming the performance index $J_1(y)$, obtained by any arbitrary stable control scheme, and the perfect control-related index $J_0(y)$, we can state that the following relation

$$J_0(y) \leq J_1(y), \tag{23}$$

always holds. In fact, the perfect control law ensures the globally lowest value of the mentioned norm. This obvious property is also confirmed here, since the control error tends to zero for any $t > dt \to 0$ [14].

Remark 6: The employment of $\mathbf{B}^{\mathrm{R}}$ and $\mathbf{C}^{\mathrm{R}}$ in our investigation exhausts successfully the set of right-invertible plants $(\mathbf{CB})^{\mathrm{R}}$.

Having defined this particular control law, let us discuss the stability behavior for the new continuous-time perfect control framework.

V. STABILITY PROPERTIES OF NEW PERFECT CONTROL LAW

The stability of CTPC algorithm is a complex problem worth of separate investigation. In this section, a brief investigation on this matter is made in order to stress out of possible difficulties. At the very beginning it is noteworthy, that the stability in the perfect control approach should be understood in the terms of bounded-input, bounded-output (BIBO) technique or even BIBS (bounded-input, bounded-state) methodology. This is supported by the fact, that the output variables reach the reference value in possible no time, with the guaranteed stable output behavior. The stability of perfect control is clearly connected with the closed-loop poles, calculated according to the state-feedback formula

$$eig(\mathbf{A} - \mathbf{BK}). \tag{24}$$

In such BIBO/BIBS paradigms, only the auto-regressive parts of the system dynamics are taken into consideration, with the well-known criterion covering connection between closed-loop poles and discussed the stability feature. Studies concerning the discrete-time perfect control systems have shown, that the state-feedback matrix $\mathbf{K}$ used in this control design is crucial in the context of obtaining the different closed-loop poles [14]. For example, the application of nonunique matrix inverses can lead to the different control properties with various closed-loop system matrix [11]. Interestingly, in all perfect-applicable nonsquare instances at least single zero pole has been obtained [14]. As long as in the discrete-time framework a pole located in the origin of the complex plane is not an issue, the continuous-time zero pole is unsatisfactory. Unfortunately, this property cannot be tackled for now, thus the stability shall be determined basing on the nonzero closed-loop control plant poles.

When we consider the issue of CTPC stability in the context of BIBO approach, it has analytically been proven and confirmed by the simulation tests that the proposed perfect control is stable through the crucial matrix $\mathbf{M}$. Observe, that the mentioned structure depend not only on constant fixed values, but it takes into account signals that are changing during the control process (see expression (16)). Indeed, the form of relation (16) could imply that the $\mathbf{M}$ is time-variant even for a constant reference value $\mathbf{y_{ref}}(t)$. However, the conducted investigation has shown that the matrix $\mathbf{M}$ can only be defined by two unique forms. This fact is summarized by the following theorem.

Theorem 2: For a steady reference value $\mathbf{y_{ref}}(t) = \mathbf{y_{ref}}$, the CTPC law as in (15) is stable through the matrix $\mathbf{M}$ associated with only two operating time ranges. The first scenario is determined by the initial conditions, whereas the second one employs the matrix $\mathbf{M} = \mathbf{0}$.

Proof: In the first time range $\langle t_0, t_1)$, where $t_1 = t_0 + dt$ for $dt \to 0$ and $\mathbf{y}(t_0) = \mathbf{Cx}(t_0)$ corresponds to the initial condition, we end up with the $\mathbf{M}$-related energy inclusion providing $\mathbf{y}(t_1) = \mathbf{y_{ref}}(t_1)$ (see framework (15-19)). However, the second range $\langle t_1, +\infty)$ excludes the matrix $\mathbf{M}$ because of

$$\mathbf{M} = \mathbf{C}^{\mathrm{R}}\frac{1}{dt}\left[\underbrace{\mathbf{Cx}(t_{k-1}) - \mathbf{y_{ref}}(t_k)}_{\mathbf{0}}\right]\mathbf{x}^{\mathrm{L}}(t_{k-1}) = \mathbf{0}, \tag{25}$$

under $\mathbf{Cx}(t_1) = \mathbf{y_{ref}}(t)$. Thus, the expression (15) reduces to

$$\mathbf{u}(t) = -(\mathbf{CB})^{\mathrm{R}}\mathbf{CAx}(t), \tag{26}$$

which provides

$$\dot{\mathbf{x}}(t) = \left(\mathbf{A} - \mathbf{B}(\mathbf{CB})^{\mathrm{R}}\mathbf{CA}\right)\mathbf{x}(t). \tag{27}$$

Finally, assuming the relation (9) we receive

$$\mathbf{x}(t_k) = \left(\mathbf{I}_n + \left(\mathbf{A} - \mathbf{B}(\mathbf{CB})^{\mathrm{R}}\mathbf{CA}\right)dt\right)\mathbf{x}(t_{k-1}), \tag{28}$$

and

$$\mathbf{y}(t_k) = \mathbf{Cx}(t_k), \tag{29}$$

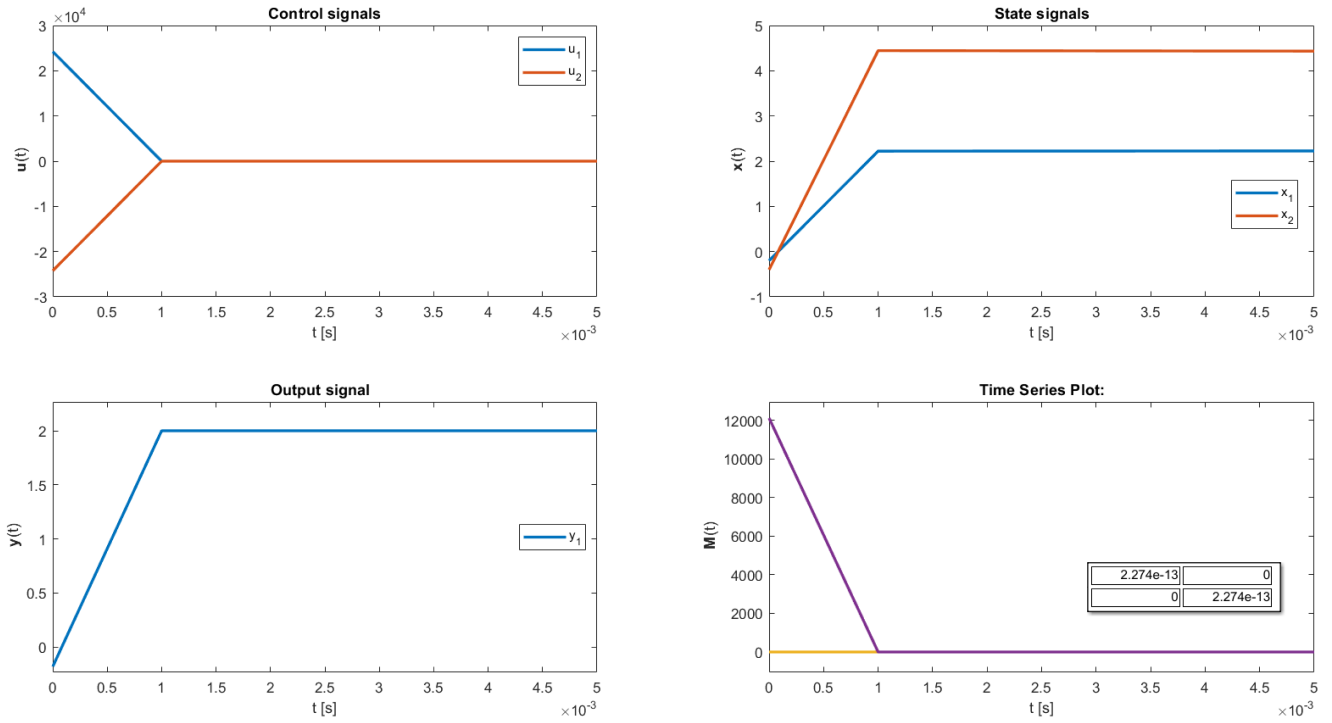

FIGURE 2. Continuous-time perfect control of the two-by-one system.

determining

$$\mathbf{y}(t_k) = \left(\mathbf{C} + \left(\underbrace{\mathbf{CA} - \underbrace{\mathbf{CB}(\mathbf{CB})^{\mathrm{R}}}_{\mathbf{I}_{n_y}} \mathbf{CA}}_{\mathbf{0}} \right) dt \right) \mathbf{x}(t_{k-1}) = \mathbf{Cx}(t_{k-1}) = \mathbf{y_{ref}}(t_k), \tag{30}$$

what ends the proof.

□

Remark 7: Naturally, in the case of a time-varying reference value, the same paradigm has occurred. Nevertheless, the discussed two operating time ranges should be respected to the two neighboring setpoint samples in this scenario.

Remark 8: Still, the analytical statement covering the stability-related characteristic equation is pursued, what constitutes the solid perfect control open problem.

After introduction of the new perfect control procedure, let us switch now to the simulation examples in the next section. The numerical tests clearly show the advantages of the new peculiarities.

VI. SIMULATION EXAMPLES

At the beginning, it should be indicated that a plethora of numerical instances have been performed in order to highlight the outstanding properties of the new approach. Among examples, two representative ones have been selected, finally to obtain a solid proof-related background. The first stable instance has employed the reduced expression (20). On the other hand, the second practical scenario providing the control of the plotter robot is derived from the application of the more complex relation (16). We start with two-input single-output plant.

A. TWO-BY-ONE STABLE SYSTEM

Consider the continuous-time state-space system with two inputs, one output and two state variables as follows

$$\mathbf{A} = \begin{bmatrix} 0.1 & 0.2 \\ -0.3 & -0.4 \end{bmatrix}, \ \mathbf{B} = \begin{bmatrix} 0.2 & 0.1 \\ 0.5 & 0.3 \end{bmatrix}, \mathbf{C} = \begin{bmatrix} 0.5 & 0.2 \end{bmatrix}, \tag{31}$$

with the initial condition $\mathbf{x_0} = [-0.2 \ -0.4]^{\mathrm{T}}$. As we can see, the plant is stable according to $eig(\mathbf{A}) = [-0.1 \ -0.2]^{\mathrm{T}}$. Additionally observe, that after using the perfect control law (15), we receive the reference value $\mathbf{y_{ref}}(t) = 2$ just after one simulation step equal to $dt = 0.001$s. The Fig. 2 clearly confirms the correctness of the innovative control algorithm. In fact, for time predictor $t \geq d = 1$ the output reaches the assumed setpoint.

On the other hand, the stable matrix $\mathbf{M}_{2\times 2}$ is expressed by two operating time ranges examined previously. Its value, derived from the reduced relation (20), depicts the Fig. 2 (down right corner). Of course, the nonzero pieces in t_0 are associated with the initial condition $\mathbf{x}_0$. It is also amazing

that the sequence of time samples switches to the respective stability-oriented formulations as follows

$$\begin{aligned}\Gamma_1 &= eig\left(\mathbf{A}-\mathbf{B}(\mathbf{CB})^{\mathrm{R}}_{\sigma}\Big|_{\underline{\beta}}\mathbf{CA}-\mathbf{M}\right)\Big|_{t=t_0}\\ &= [-1.21\ \ -1.21]^{\mathrm{T}} * 10^4, \qquad (32)\\ \Gamma_2 &= eig\left(\mathbf{A}-\mathbf{B}(\mathbf{CB})^{\mathrm{R}}_{\sigma}\Big|_{\underline{\beta}}\mathbf{CA}\right)\Big|_{t\geq t_1}\\ &= [0\ \ -0.34]^{\mathrm{T}}, \qquad (33)\end{aligned}$$

providing the strictly stable region only in the first case ($s_1 = -1.21 * 10^4$, $s_2 = -1.21 * 10^4$). However, the expression Γ_2 locates the closed-loop perfect control pole at zero, finally to obtain $s_1 = 0$ and $s_2 = -0.34$. It should be emphasized, that the presented study has been performed with application of $\underline{\beta} = [3\ \ 1]$ substituted into the generalized σ-inverse of the matrix product $\mathbf{CB}$ (for instance see (6)). The zero-related detrimental poles can probably be excluded in terms of employment of other nonunique right inverses, what provides a really serious problem in the future.

In another simulation example the more complex practical plant is deeply investigated.

B. 3D PLOTTER ROBOT

In order to demonstrate the practical involvement of the innovative CTPC procedure, let us consider the Cartesian coordinate robot working in 3D-space presented in Fig. 3.

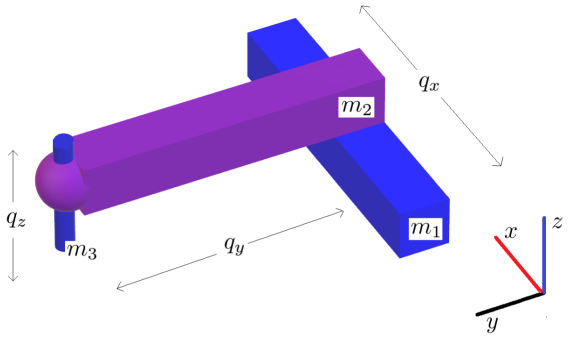

FIGURE 3. 3D plotter robot diagram.

Observe, that the dynamic properties of the discussed robot can be described in according to the Euler-Lagrange-originated relations as follows

$$\begin{cases}\dfrac{d}{dt}\left(\dfrac{\partial L}{\partial \dot{q}_x}\right)-\dfrac{\partial L}{\partial q_x}=F_x-k_x\dot{q}_x\\ \dfrac{d}{dt}\left(\dfrac{\partial L}{\partial \dot{q}_y}\right)-\dfrac{\partial L}{\partial q_y}=F_y-k_y\dot{q}_y\\ \dfrac{d}{dt}\left(\dfrac{\partial L}{\partial \dot{q}_z}\right)-\dfrac{\partial L}{\partial q_z}=F_z-k_z\dot{q}_z,\end{cases} \qquad (34)$$

where set $\Omega = \{q_x, q_y, q_z\}$ stands for the gripper tip position. The symbols F_x, F_y and F_z denote the forces of respective x, y and z axes, whereas k_x, k_y and k_z define the viscous frictions. Moreover, the difference L between kinetic T and potential U energies can be calculated in the subsequent manner

$$\begin{aligned}L = T\text{-}U &= \frac{1}{2}(m_1+m_2+m_3)\dot{q}_x{}^2(t)\\ &+\frac{1}{2}(m_2+m_3)\dot{q}_y{}^2(t)+\frac{1}{2}m_3\dot{q}_z{}^2(t)\\ &-m_3gq_z. \qquad (35)\end{aligned}$$

Thus, after combining the formulas (34) and (35) we obtain the final form of the crucial dynamics

$$\begin{cases}\ddot{q}_x(t) = -k'_x\dot{q}_x(t)+\dfrac{1}{m_1+m_2+m_3}F_x\\ \ddot{q}_y(t) = -k'_y\dot{q}_y(t)+\dfrac{1}{m_2+m_3}F_y\\ \ddot{q}_z(t) = -k'_z\dot{q}_y(t)+\dfrac{1}{m_3}F'_z,\end{cases} \qquad (36)$$

where $k'_x = k_x/(m_1+m_2+m_3)$, $k'_y = k_x/(m_2+m_3)$, $k'_z = k_z/m_3$ and $F'_z = F_z + m_3g$.

Following the notion, the expression (36) can be transformed to the well-known state-space representation as follows

$$\begin{bmatrix}\ddot{q}_x(t)\\ \ddot{q}_y(t)\\ \ddot{q}_z(t)\end{bmatrix} = \begin{bmatrix}-k'_x & 0 & 0\\ 0 & -k'_y & 0\\ 0 & 0 & -k'_z\end{bmatrix}\begin{bmatrix}\dot{q}_x(t)\\ \dot{q}_y(t)\\ \dot{q}_z(t)\end{bmatrix} + \begin{bmatrix}\dfrac{1}{m_1+m_2+m_3} & 0 & 0\\ 0 & \dfrac{1}{m_2+m_3} & 0\\ 0 & 0 & \dfrac{1}{m_3}\end{bmatrix}\begin{bmatrix}F_x\\ F_y\\ F'_z\end{bmatrix}. \qquad (37)$$

What is more, the output equation in the form of

$$\mathbf{y}(t) = \begin{bmatrix}1 & 1 & 0\\ 0 & 0 & 1\end{bmatrix}\begin{bmatrix}\dot{q}_x(t)\\ \dot{q}_y(t)\\ \dot{q}_z(t)\end{bmatrix}, \qquad (38)$$

guarantees the reference values/setpoints on the vector of speed resultant derived from the XY-plane and the vertical velocity vector strictly associated with the Z-axis.

Thus, having the essential peculiarities we can write, for the selected parameters $k'_x = 0.4$, $k'_y = 0.3$, $k'_z = 0.1$, $m_1 = 0.1$, $m_2 = 0.4$ and $m_3 = 0.5$, the state-space-oriented triplet $S(\mathbf{A}, \mathbf{B}, \mathbf{C})$ expressed as

$$\mathbf{A} = \begin{bmatrix}-0.4 & 0 & 0\\ 0 & -0.3 & 0\\ 0 & 0 & -0.1\end{bmatrix},\ \mathbf{B} = \begin{bmatrix}1 & 0 & 0\\ 0 & 2 & 0\\ 0 & 0 & 2\end{bmatrix},\ \mathbf{C} = \begin{bmatrix}1 & 1 & 0\\ 0 & 0 & 1\end{bmatrix}. \qquad (39)$$

Observe, that according to the $eig(\mathbf{A}) = [-0.4\ \ -0.3\ \ -0.1]^{\mathrm{T}}$, the discussed real-life system is stable. Now, taking into account the complex more general CTPC law (16),

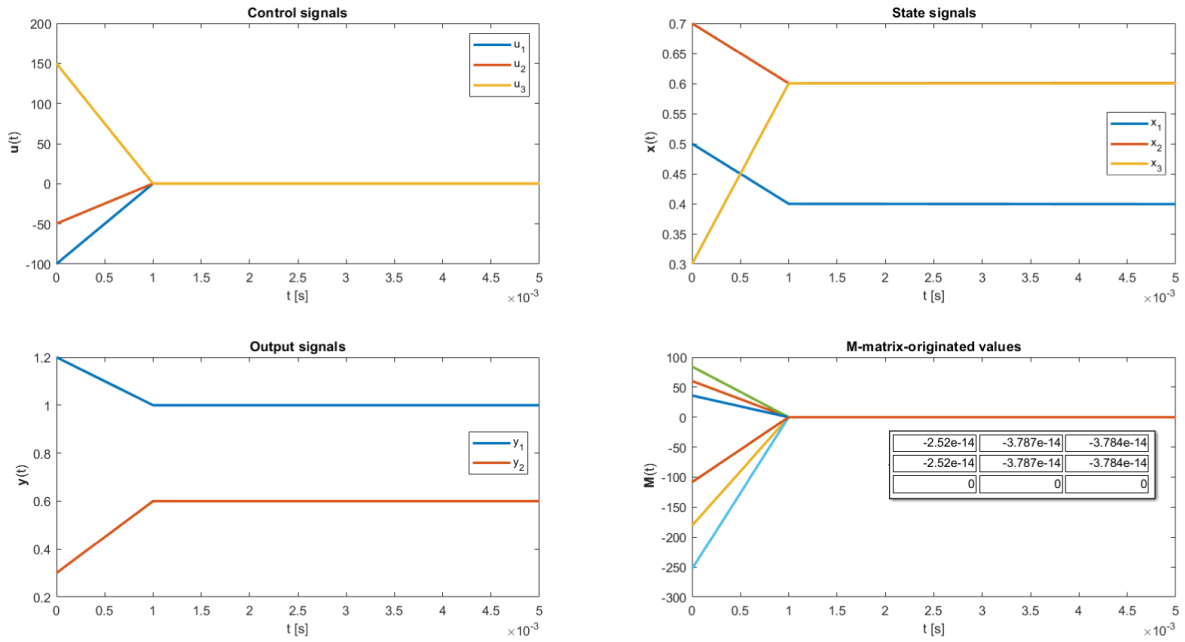

FIGURE 4. Continuous-time perfect control of the 3D plotter robot.

we receive the expected signal runs depicted in Fig. 4. The plant's output reaches the reference value $\mathbf{y_{ref}}(t) = [1 \quad 0.6]^{\mathrm{T}}$ after one-step delay equal to $dt = 0.001$s. Naturally, this outcome is supported by the randomly chosen initial state vector $\mathbf{x_0} = [0.5 \;\; 0.7 \;\; 0.3]^{\mathrm{T}}$ and arbitrary selected degrees of freedom matrix

$$\underline{\beta} = \begin{bmatrix} 4 & -1 & 6 \\ 3 & 2 & 4 \end{bmatrix}. \tag{40}$$

Finally, it should be emphasized that the new CTPC method is still valid for any time-varying setpoint trajectory and every continuous step time dt. Again, the correctness of the innovative perfect control procedure along with the widely understood application potential has been confirmed. It has been done here by the authors' real-life robot-related object.

VII. CONCLUSION AND OPEN PROBLEMS

In the paper, the new perfect control algorithm dedicated to LTI multivariable continuous-time systems in the state-space framework is proposed. The control law meets all requirements associated with its previous discrete-time instance. It would be very interesting to solve the perfect control stability problem with other, than the BIBO criterion, complex analytical statement. Moreover, the employment of a number of generalized inverses could be helpful in such innovative investigations. In the end, the application of the new procedure to the nonlinear real-life objects seems to be welcomed. Naturally, in order to guarantee this practical complex requirement, a new nonlinear instance of the perfect control strategy in the continuous-time domain should immediately be introduced.

REFERENCES

[1] W. P. Hunek and T. Feliks, "A new geometric-oriented minimum-energy perfect control design in the IMC-based state-space domain," *IEEE Access*, vol. 8, pp. 41733–41739, 2020.

[2] T. L. Molloy, J. Inga, M. Flad, J. J. Ford, T. Perez, and S. Hohmann, "Inverse open-loop noncooperative differential games and inverse optimal control," *IEEE Trans. Autom. Control*, vol. 65, no. 2, pp. 897–904, Feb. 2020.

[3] H. Ma, M. Chen, and Q. Wu, "Disturbance observer-based inverse optimal tracking control of the unmanned aerial helicopter," in *Proc. IEEE 8th Data Driven Control Learn. Syst. Conf. (DDCLS)*, May 2019, pp. 448–452.

[4] W. P. Hunek and M. Krok, "Towards a new minimum-energy criterion for nonsquare LTI state-space perfect control systems," in *Proc. 5th Int. Conf. Control, Decis. Inf. Technol. (CoDIT)*, Thessaloniki, Greece, Apr. 2018, pp. 122–127.

[5] F. Cao, T. Yang, Y. Li, and S. Tong, "Adaptive neural inverse optimal control for a class of strict feedback stochastic nonlinear systems," in *Proc. IEEE 8th Data Driven Control Learn. Syst. Conf. (DDCLS)*, May 2019, pp. 432–436.

[6] A. Giusti, J. Malzahn, N. G. Tsagarakis, and M. Althoff, "On the combined inverse-dynamics/passivity-based control of elastic-joint robots," *IEEE Trans. Robot.*, vol. 34, no. 6, pp. 1461–1471, Dec. 2018.

[7] W. P. Hunek and K. Latawiec, "Minimum variance control of discrete-time and continuous-time LTI MIMO systems—A new unified framework," *Control Cybern.*, vol. 38, pp. 609–624, Sep. 2009.

[8] A. Ben-Israel and T. N. E. Greville, *Generalized Inverses, Theory and Applications*, 2 ed. New York, NY, USA: Springer-Verlag, 2003.

[9] N. P. Karampetakis, "On the computation of the generalized inverse of a polynomial matrix," *IMA J. Math. Control Inf.*, vol. 18, no. 1, pp. 83–97, Mar. 2001.

[10] T. Nguyen, "Inverse of a special matrix and application," 2017, *arXiv:1708.07795*. [Online]. Available: https://arxiv.org/abs/1708.07795

[11] M. Krok and W. P. Hunek, "Pole-free perfect control: Theory vs. Simulation examples," in *Proc. 23rd Int. Conf. Methods Models Automat. Robot. (MMAR)*, Międzyzdroje, Poland, Aug. 2018, pp. 199–204.

[12] X. Lin, C. Wu, and B. Chen, "Robust H_∞ adaptive fuzzy tracking control for MIMO nonlinear stochastic Poisson jump diffusion systems," *IEEE Trans. Cybern.*, vol. 49, no. 8, pp. 3116–3130, Jun. 2019.
[13] P. Navratil, L. Pekar, and R. Matusu, "Control of a multivariable system using optimal control pairs: A quadruple-tank process," *IEEE Access*, vol. 8, pp. 2537–2563, 2020.
[14] W. P. Hunek and M. Krok, "A study on a new criterion for minimum-energy perfect control in the state-space framework," *Proc. Inst. Mech. Eng., I, J. Syst. Control Eng.*, vol. 233, no. 7, pp. 779–787, 2019.
[15] J. Wu and Y. Lu, "Decoupling and optimal control of multilevel buck DC–DC converters with inverse system theory," *IEEE Trans. Ind. Electron.*, vol. 67, no. 9, pp. 7861–7870, Sep. 2020.
[16] Y. Li, Y. Yao, and X. Hu, "Continuous-time inverse quadratic optimal control problem," *Automatica*, vol. 117, Jul. 2020, Art. no. 108977.
[17] J. Klamka, "Controllability and minimum energy control problem of fractional discrete-time systems," in *New Trends in Nanotechology and Fractional Calculus Applications*, D. Baleanu, Z. B. Guvenc, and J. A. T. Machado, Eds. Heidelberg, Germany: Springer, 2010, pp. 503–509.
[18] J. Liu, Y. Liang, and N. Ansari, "Spark-based large-scale matrix inversion for big data processing," *IEEE Access*, vol. 4, pp. 2166–2176, 2016.
[19] T. Britz, "The Moore-Penrose inverse of a free matrix," *Electron. J. Linear Algebra*, vol. 16, pp. 208–215, Jan. 2007.
[20] B. Zhang and J. Uhlmann, "A generalized matrix inverse with applications to robotic systems," 2018, *arXiv:1806.01776*. [Online]. Available: https://arxiv.org/abs/1806.01776
[21] G.-P. Liu and S. Zhang, "A survey on formation control of small satellites," *Proc. IEEE*, vol. 106, no. 3, pp. 440–457, Mar. 2018.
[22] A. Ibanez, P. Bidaud, and V. Padois, "Emergence of humanoid walking behaviors from mixed-integer model predictive control," in *Proc. IEEE/RSJ Int. Conf. Intell. Robots Syst.*, Sep. 2014, pp. 4014–4021.
[23] M. Jiang, B. Jiang, and Q. Wang, "Internal model control for rank-deficient system with time delays based on damped pseudo-inverse," *Processes*, vol. 7, no. 5, p. 264, May 2019.
[24] L. R. E. Shead, C. G. Anastassakis, and J. A. Rossiter, "Steady-state operability of multi-variable non-square systems: Application to model predictive control (MPQ of the shell heavy oil fractionator (SHOF)," in *Proc. Medit. Conf. Control Automat.*, Athens, Greece, Jun. 2007, pp. 1–6.
[25] P. Chen, L. Ou, D. Gu, and W. Zhang, "Robust analytical scheme for linear non-square systems," in *Proc. 48h IEEE Conf. Decis. Control (CDC)*, Dec. 2009, pp. 1890–1895.
[26] K. L. N. Sarma and M. Chidambaram, "Centralized PI/PID controllers for nonsquare systems with RHP zeros," *Indian Inst. Sci.*, vol. 85, no. 4, pp. 201–214, 2005.
[27] E. J. Loh and M.-S. Chiu, "Robust decentralized control of non-square systems," *Chem. Eng. Commun.*, vol. 158, no. 1, pp. 157–180, Apr. 1997.
[28] S. Kolavennu, S. Palanki, and J. C. Cockburn, "Nonlinear control of nonsquare multivariable systems," *Chem. Eng. Sci.*, vol. 56, no. 6, pp. 2103–2110, Mar. 2001.
[29] S. J. Shiu, C. C. Yu, and S. H. Shen, "Multivariable control of multizone chemical mechanical polishing," *J. Vac. Sci. Technol. B, Microelectron. Nanometer Struct.*, vol. 22, no. 4, pp. 1679–1687, 2004.
[30] H. Gluesing-Luerssen, J. Rosenthal, and R. Smarandache, "Strongly-MDS convolutional codes," *IEEE Trans. Inf. Theory*, vol. 52, no. 2, pp. 584–598, Feb. 2006.
[31] S. Wahls, H. Boche, and V. Pohl, "Zero-forcing precoding for frequency selective MIMO channels with criterion and causality constraint," *Signal Process.*, vol. 89, no. 9, pp. 1754–1761, Sep. 2009.
[32] L. Zhang and A. Makur, "Multidimensional perfect reconstruction filter banks: An approach of algebraic geometry," *Multidimensional Syst. Signal Process.*, vol. 20, no. 1, pp. 3–24, Mar. 2009.
[33] T. E. Tuncer, "Deconvolution and preequalization with best delay LS inverse filters," *Signal Process.*, vol. 84, no. 11, pp. 2207–2219, Nov. 2004.
[34] M. Castella and J. C. Pesquet, "An iterative blind source separation method for convolutive mixtures of images," in *Independent Component Analysis and Blind Signal Separation*, C. G. Puntonet and A. Prieto, Eds. Berlin, Germany: Springer, 2004, pp. 922–929.
[35] W. P. Hunek and P. Majewski, "Perfect reconstruction of signal—A new polynomial matrix inverse approach," *EURASIP J. Wireless Commun. Netw.*, vol. 2018, no. 1, pp. 1–8, Dec. 2018.
[36] W. P. Hunek and P. Dzierwa, "New results in generalized minimum variance control of computer networks," *Inf. Technol. Control*, vol. 43, no. 3, pp. 315–320, Sep. 2014.
[37] K. Tchoń, J. Karpińska, and M. Janiak, "Approximation of jacobian inverse kinematics algorithms," *Int. J. Appl. Math. Comput. Sci.*, vol. 19, no. 4, pp. 519–531, Dec. 2009.
[38] T. Zhang, H. G. Li, Z. Y. Zhong, and G. P. Cai, "Hysteresis model and adaptive vibration suppression for a smart beam with time delay," *J. Sound Vibrat.*, vol. 358, pp. 35–47, Dec. 2015.
[39] D. Horla and A. Krolikowski, "Continuous-time adaptive LQG/LTR control," *IFAC Proc. Volumes*, vol. 45, no. 13, pp. 559–563, 2012.
[40] T. Kaczorek, "Cayley–Hamilton theorem for fractional linear systems," in *Theory and Applications of non-Integer Order Systems*, A. Babiarz, A. Czornik, J. Klamka, and M. Niezabitowski, Eds. Cham, Switzerland: Springer, 2017, pp. 45–55.
[41] Z. Tan, L. Xiao, S. Chen, and X. Lv, "Noise-tolerant and finite-time convergent ZNN models for dynamic matrix Moore–Penrose inversion," *IEEE Trans. Ind. Informat.*, vol. 16, no. 3, pp. 1591–1601, Mar. 2020.
[42] A. M. Ahmadian, W. Zirwas, R. S. Ganesan, and B. Panzner, "Low complexity Moore-Penrose inverse for large CoMP areas with sparse massive MIMO channel matrices," in *Proc. IEEE 27th Annu. Int. Symp. Pers., Indoor, Mobile Radio Commun. (PIMRC)*, Sep. 2016, pp. 1–7.
[43] M. V. D. Nair, R. Giofre, P. Colantonio, and F. Giannini, "NARMA based novel closed loop digital predistortion using Moore-Penrose inverse technique," in *Proc. 11th Eur. Microw. Integr. Circuits Conf. (EuMIC)*, Oct. 2016, pp. 405–408.
[44] M. T. Hanna, "The revised direct batch evaluation algorithm of optimal eigenvectors of the DFT matrix using the notion of Moore-Penrose matrix pseudoinverse," in *Proc. 6th Int. Symp. Commun., Control Signal Process. (ISCCSP)*, May 2014, pp. 433–436.
[45] Y. Takane, "Relationships among various kinds of eigenvalue and singular value decompositions," in *New Developments in Psychometrics*, H. Yanai, A. Okada, K. Shigemasu, Y. Kano, and J. J. Meulman, Eds. Tokyo, Japan: Springer, 2003, pp. 45–56.

PAWEŁ MAJEWSKI received the B.Sc. degree, the M.Sc. degree in electrical engineering, and the Ph.D. degree in control engineering from the Opole University of Technology, Opole, Poland. From 2011 to 2016, he worked as a Constructor/Robot Programmer with Pawos Robotics Company. Since 2015, he has been employed with the Opole University of Technology. He is the author or coauthor of 20 articles/conference proceedings and he promoted over 30 graduates. His research interests concern the implementation of nonunique polynomial inverses in multivariable nonsquare systems.

WOJCIECH P. HUNEK received the Ph.D. and Habilitation degrees in electrical engineering and automatic control and robotics from the Faculty of Electrical, Control and Computer Engineering, Opole University of Technology, in 2003 and 2012, respectively. He is currently working as an Associate Professor with the Department of Control Engineering. He has authored or coauthored about 100 articles, most of them are concerned with the up-to-date topics in the multivariable control and systems theory.

MAREK KROK was born in Opole, Poland, in 1991. He graduated in control engineering from the Opole University of Technology, in 2015, and the Ph.D. degree in control, electronic and electrical engineering, in 2020. Since 2015, his research has been focused on a broad range of subjects associated with control theory, particularly on the application of nonunique matrix inverses in the perfect control algorithm. He has coauthored over 11 articles published in international journals and has given numerous presentations on international conferences.